Autonomous Tethered Extension Fixture (ATEF) Mission

Jack Anderson, Tyler Brazenec, Tyler Calcagni, Logan Segeda, Fotios Angelopoulos, Dev Sarvaiyya, Abdulaziz Alotaibi
Pennsylvania State University, State College, PA, 16801

Professor Sara Lego[1]
Pennsylvania State University, State College, PA, 16801

Michael Hernandez[2]
iMETALX, Sausalito, CA, 94965

The ATEF mission is designed to provide an economical and versatile satellite servicing solution, specifically targeting Low Earth Orbit platforms to extend mission lifespans. In response to the mission extension services gap left since the decommissioning of the Space Shuttle, ATEF leverages innovative materials and off-the-shelf components to augment a satellite's onboard attitude and orbit control systems. The mission employs breakthrough technologies such as nitinol, a shape memory alloy, and gecko grippers in a miniaturized docking mechanism that minimizes mass and power consumption while ensuring robust performance. ATEF is engineered to execute semi-autonomous rendezvous and docking with non-cooperative targets, with Hubble serving as a primary docking candidate due to its accessible design data and the fact that NASA is actively looking into send up a servicing mission to restore its failing control moment gyros. The system architecture incorporates detailed analyses of the docking, structural, C&DH, thermal, power, communication, attitude, and propulsion subsystems along with extensive fault and risk management strategies to ensure safety and reliability under demanding operational conditions. Overall, ATEF promises to bridge a critical gap in satellite servicing by offering a cost-effective alternative capable of enhancing satellite functionality, reducing lifecycle costs, and adapting seamlessly to a wide range of LEO assets.

Nomenclature

α	=	Absorptivity
A_f	=	Albedo factor
$A_{1,2,etc.}$	=	Surface areas
ε or $\epsilon_{1,2,}$	=	Emissivity of a material
$F_{1\to 2}$	=	Viewing factor
k	=	Thermal conductivity
Q	=	Heat transfer
S	=	Solar constant
t	=	Thickness
$T_{1,2,etc.}$	=	Temperatures in of a material
T_E	=	Black body temperature of the Earth
θ	=	Incident angle between the normal solar vector and the solar vector
σ	=	Stefan-Boltzmann constant

I. Introduction

Ever since the decommissioning of the Space Shuttle, the space industry has lacked a reliable method to replace failing control moment gyroscopes and reaction wheels, a shortfall that has resulted in the early termination of several satellite missions. This gap in satellite servicing capability has not only led to premature mission terminations but has also created a significant market opportunity. Northrop Grumman estimates that servicing missions targeting geostationary (GEO) satellites alone could represent a market worth approximately $3.2 billion by 2030[1]. Currently, the only existing solution to extend satellite lifetime is Northrop Grumman's Mission Extension Vehicles, MEV-1 and MEV-2. These platforms are designed to dock with a failing satellite and take over certain critical functions, effectively extending the satellite's operational life. The MEV achieves this by latching onto

1 – Associate Teaching Professor, Aerospace Engineering, 374 ECoRE Building, State College, PA, 16801
2 – Senior GNC Engineer: Space Systems Architect, 2350 Marinship Way Building 9, Sausalito, CA 94956

standard liquid apogee engines and then using its onboard systems to provide the necessary attitude and orbit control for the target satellite[1].

Unfortunately, the MEV has not filled the service capability gap in Low Earth Orbit (LEO) due to its large size and cost, which limits it to operations only in GEO, where many high value targets are very close by in delta-V terms. ATEF fills this capability gap by using innovative materials and off-the-shelf components to build a cost-effective servicing mission. By utilizing shape memory alloys, gecko grippers, and a much smaller vehicle, ATEF can rendezvous and dock with LEO satellites, augmenting the attitude and orbital control of the target satellite without the need for any particular docking hardware on the target spacecraft.

II. Mission Overview

The primary purpose of the ATEF mission is to extend the operational lifespans of satellites in LEO. Specifically, ATEF aims to provide existing LEO satellites with an affordable option to supplement their onboard attitude and orbit control systems, thereby prolonging their mission life. To achieve this ATEF will conduct the following key operation:

1. Perform Semi-Autonomous Rendezvous and Docking: Ensure that the payload can semi-autonomously locate and securely dock with the target satellite, regardless of whether the satellite is cooperative.
2. Establish a Secure Connection: Utilize a docking system capable of withstanding operational forces while providing a reliable platform for subsequent integration tasks.
3. Integrate with the target satellite's AOC system: Enable communication between the payload and the satellite to synchronize control systems via ground-uploaded software.
4. Conduct Operational Validation: Execute post-docking tests to verify that the payload effectively maneuvers the satellite and fulfills its intended purpose.
5. Move to Nominal Operations: Supplement the targets AOC system until a designated EOL.

A. Atef's Innovations:

ATEF excels in efficiency, miniaturization, and universality. Operating on the Venus Class Bus, it consumes 22.5 times less power, weighs 15 times less, and is 25 times smaller than competing solutions[1] thanks to breakthroughs with nitinol and gecko grippers. These advances reduce the size of key components such as solar panels and docking hardware, thus lowering the overall mass compared to the MEV and dramatically cutting launch costs. To put this into perspective, it is possible to launch upwards of 60 ATEF missions to LEO on one Falcon 9[2]. Its streamlined design uses readily available or in-house machined parts, making production cost-effective, which helps further bring down the cost of the mission. Additionally, ATEF's unique docking mechanism can interface with almost any satellite with minimal modifications, proving it as a cost-effective and versatile solution for satellites in LEO.

B. Selection of a Docking Target:

The team is selecting the Hubble space telescope as ATEF's docking target for several key reasons. Hubble is publicly known for experiencing pointing system failure[3] and has a wide availability of CAD models and schematics[4]. Furthermore, NASA has expressed interest in sending a mission extension package to Hubble[5]. This would be fitting for ATEF due to Hubble's size and surfaces, which are ideal for testing ATEF's docking method, along with its accessible position in LEO. While Hubble is not strictly necessary to prove ATEF's capabilities, it offers the most practical target. Now if NASA were to not approve of this mission, a small micro satellite demonstrator could be launched with ATEF and then be used as the docking target.

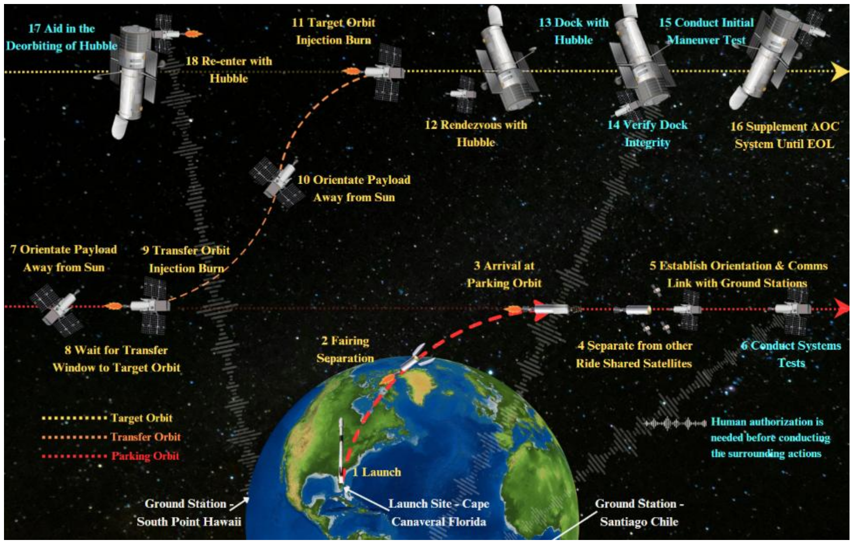

Figure 1. Macro Level Mission Architecture.

Table 1. Payload Mass Budget.

Payload Deatiled Mass Budget		
Payload Subsystem	Part Name	Mass (kg)
Structure	Main Body	9.58
Structure	Top Plate	2.26
Thermal	Aluminized Mylar	0.031
Docking	Nitinol Bands x 12	1.26
Docking	Kevlar Insulation	0.75
Docking	MLI Outer Insulation	0.023
Docking	Geck Grippers	0.38
Docking	Central Bus	3.3
C&DH	NovAtel OEM719	0.031
C&DH	Ouser OS1	0.43
C&DH	IM200	0.059
Total Payload Mass		18.1
Contingency Mass		3.62
Design Reserve Mass		48.28

Table 2. Venus Class Bus Mass Budget.

Detailed X-Sat Venus Class Bus Mass Budget		
Subsystem	Part Name	Mass (kg)
Structural Mass	Aluminum 6061	77.41
Propulsion	MONARC-5	0.98
Propulsion	B1 Cold Gas Thruster x12	3.12
Propulsion	Hydrazine	10
Propulsion	N2O and C3H6	5
Thermal	Aluminized Mylar	0.578
Thermal	TMT Radiator	6.71
Power	LG MJ1 3.5Ah Battery	1.72
Power	Ibeos Modular Power System	1.1
Attitude	FleXcore	4.4
Structure	Bus Shell (Estamate)	43
C&DH	Processing Hardware	5.65
Comms	Antenna	0.049
Comms	Telemetry Interface Board	0.1
Comms	Cabling	0.09
Comms	Transmitter	0.2
Comms	Misc Components	0.1
Total Buss Mass		160.20
Total Spacecraft Mass		178.30

Table 3. Payload and Venus Class Bus Power Budget.

Payload Detailed Power Budget		
Subsystem	Part Name	Power (W)
Docking	Nitinol Bands	48.1
C&DH	NovAtel OEM719	0.9
C&DH	Ouser OS1	16
C&DH	IM200	1
X-Sat Venus Class Bus Detailed Power Budget		
Propulsion	MONARC-5	18
Propulsion	B1 Cold Gas Thruster x12	57.6
Thermal	TMT Radiator	7.8
Power	LG MJ1 3.5Ah Battery	1.8
Power	Ibeos Modular Power System	2.3
Attitude	FleXcore	18.1
C&DH	Processing Hardware	26.9
Comms	Antenna	4.6
Comms	Telemetry Interface Board	3.8
Comms	Cabling	0.4
Comms	Transmitter	7.6
Comms	Misc Components	0.3
Total Mission Power (W)		215.1
Contingency Power (W)		53.8
Initial Design Reserve (W)		175.2
EOL Desgin Reserve (W)		157.7

III. Payload Design

A. Three View of The ATEF Payload

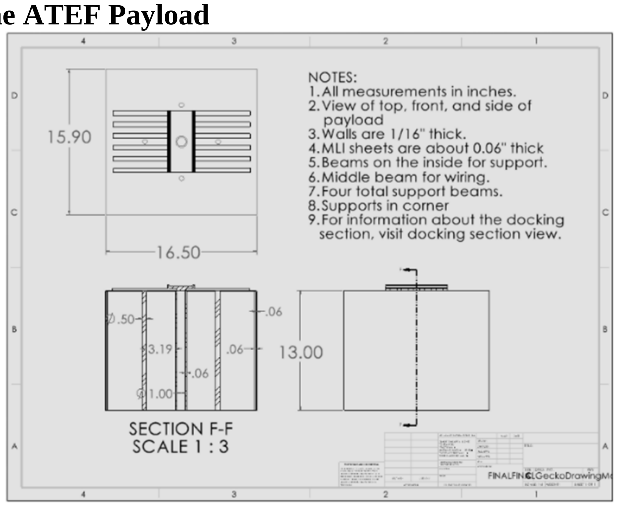

Figure 2. 3-View of the ATEF Payload.

B. Micro Level Mission Architecture

Figure 3. Micro Level Mission Architecture.

C. Docking Subsystem

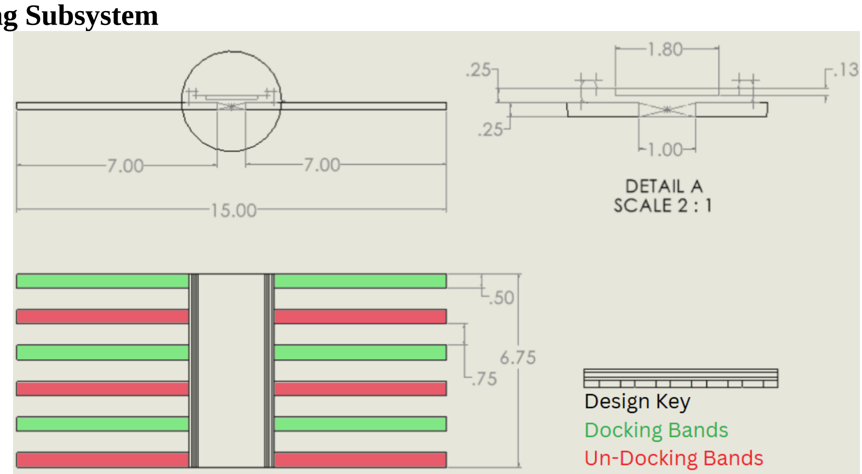

Figure 4. 3-View of the Docking Mechanism

The current docking subsystem design uses a nitinol docking clamp composed of twelve bands, each measuring 150 mm by 4 mm by 25 mm[6]. Six bands are dedicated to docking and six to undocking, all interconnected through a Kevlar mesh to function as a single surface. The docking bands are pre-molded to their "set" state so that, when heated to their activation point, they automatically clamp around the target docking point[6]. Prior to launch, these bands are flattened to lie flush with the payload's top surface Upon arrival, a current heats the docking bands to trigger their shape-memory effect. Simultaneously, this activation pulls the still inactive undocking bands, to match the set shape of the docking bands. If undocking is necessary, the same process would happen in reverse, with the undocking bands now pulling the docking bands.

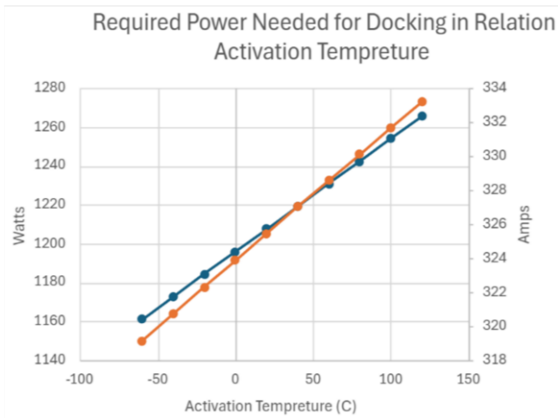

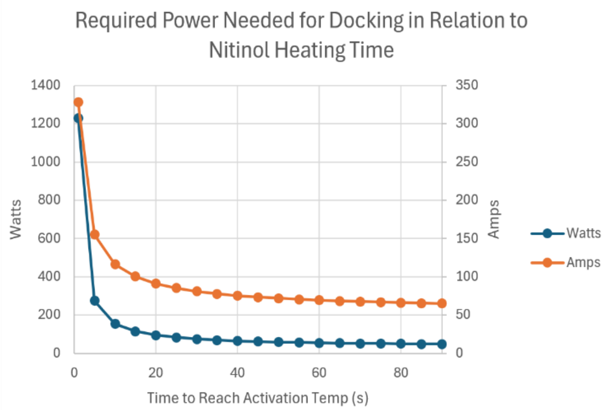

Figure 5. Power for Docking vs. Activation Temp. **Figure 6. Power vs. Time to Activation (right).**

Extensive thermal and electrical analysis were conducted to determine the optimal activation temperature for nitinol. Although increasing the activation temperature requires more energy to activate the material, a higher temperature is preferred because it reduces the risk of premature activation from solar heat and facilitates undocking easier by lowering the bending resistance of the inactive bands. Nitinol exhibits two phases: the inactive martensite phase, where its yield strength can be as low as 70 MPa[7], and the active austenite phase, where its yield strength can reach up to 690 MPa[8]. Since only half of the bands are active at any time, it is desirable to keep the inactive bands as far below the activation temperature as possible to maintain low yield strength and ease bending. Although a higher activation temperature increases energy consumption, the thermal analysis showed that the total power required to activate nitinol changes minimally over time. While the required Wattage decreases favorably with extended activation time, the current demand remains high. To resolve this, the design incorporates additional high-capacity batteries for the docking procedure, ensuring that the high current draw remains within the capabilities of onboard power sources. Ultimately, the team selected a nitinol alloy with an activation temperature of 120 °C, which requires roughly 50 watts and 67 amps over a 90-second period to dock. It is important to note that for the analysis of this section, the nitinol bands were modeled as a resistive wire which lost 3 percent of its heat per second as outlined by the nitinol manufacturer Kellogg's Research Labs[9].

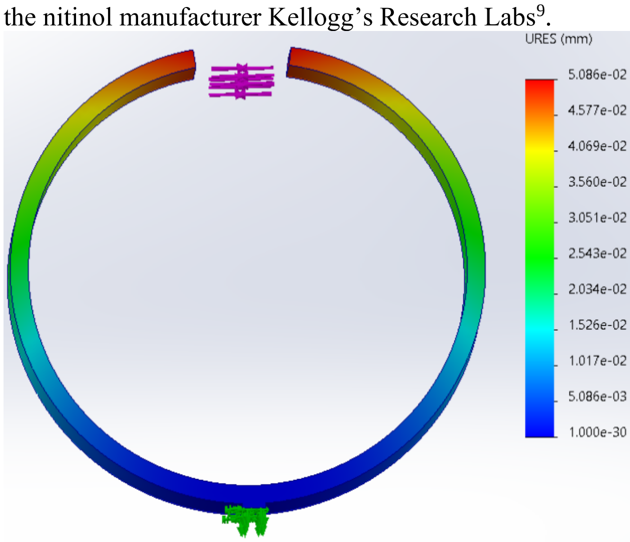

The next step of the payload design was to ensure that the nitinol provides sufficient structural support when closed so that no bending occurs during GNC support operations. Shown to the left is a model of a single nitinol band, where a 1 N force was applied along both open ends, pushing outward. This 1 N force was selected so that the bands collectively resist a total force of 12 N, which exceeds the approximately 10 N force the team expects ATEF to exert on the target. The results of this finite element analysis demonstrated that the current thickness of the nitinol bands provides enough strength to ensure minimal deformation during nominal operations. However, the analysis also revealed that the strain is sufficient for minor slipping to be a potential concern.

Figure 7. FEA of a Nitinol Band.

As such it was deemed pertinent to develop a way to help the docking claw not slip. To combat slipping, additions to the nitinol mechanism integrates supplementary components such as gecko grippers. These grippers, inspired by the adhesive properties of gecko feet, provide an extra layer of redundancy by mitigating sliding risks and extending the range of acceptable docking targets. With a combined surface area of 50 square centimeters and a sticking force of 40 kPa[9], they can collectively resist loads of up to 200 newtons[9] of both shear and normal forces.

This redundancy is crucial because it enables the mission to proceed even if the nitinol mechanism underperforms, while also ensuring that any dock between ATEF and the Hubble is rigid.

The final step of the design for this subsystem was looking into flexible materials that were strong enough to send the bending force from the active bands to the inactive bands, while being able to withstand the 120 degrees Celsius operational temperatures of the nitinol bands. As such a series of trade studies, seen below, were conducted to meet these demands.

Table 4. Docking Fabric Support Trade Study.

Docking Cross Member Frabric Support Trade Study					
	Weight	Goal	**Vectran**	**Kevlar**	**Nomex**
Modulus of Elasticity (GPa)	0.1	Max	65	112	32
Normalized Value			0.041	0.1	0
Thermal Conductivity (W/(m*K)	0.3	Min	0.37	0.004	0.1
Normalized Value			0	0.3	0.221
Max Operational Use Temp °C	0.2	Max	150	250	300
Normalized Value			0	0.133	0.2
Melting Point/Char Temp °C	0.2	Max	330	500	350
Normalized Value			0	0.2	0.024
Density (g/cm²)	0.05	Min	1.47	1.44	1.38
Normalized Value			0	0.017	0.05
TRL	0.15	Max	6	8	7
Normalized Value			0	0.15	0.075
Total	1		**0.0413**	**0.9**	**0.570**

Table 5. Docking Insulator Trade Study.

Docking Insulator Trade Study					
	Weight	Goal	**Aluminum Coated PET**	**Aluminum Coated Polyimide**	**Aluminum Coated Polyimide with AOC**
Solar Absorptance (α)	0.1	Min	0.14	0.14	0.14
Normalized Value			0.1	0.1	0.1
Emittance (ε)	0.2	Min	0.035	0.035	0.05
Normalized Value			0.2	0.2	0
Max Operational Temp (Intermittent) °C	0.25	Max	150	400	205
Normalized Value			0	0.25	0.055
Max Operational Temp (Continuous) °C	0.25	Max	120	290	205
Normalized Value			0	0.25	0.125
Typical Weight (g/m²) @ 1 Mill	0.05	Min	33	36	39
Normalized Value			0.05	0.025	0
TRL	0.15	Max	9	9	9
Normalized Value			0.15	0.15	0.15
Total	1		**0.5**	**0.975**	**0.43**

Kevlar and MLI were incorporated into the design to address both structural integrity and thermal management challenges. Kevlar is used to bind the nitinol bands together, ensuring that they function as a single, cohesive surface while providing high strength and extremely effective thermal insulation[10]. Meanwhile, MLI serves as a UV shield that protects the Kevlar from being damaged from UV rays while also providing additional thermal insulation[11]. Together, these materials enhance the overall reliability and performance of the docking clamp system.

Overall, the docking subsystem is designed to be robust and adaptable, utilizing proven materials like nitinol, Kevlar, and state-of-the-art insulation, while also incorporating innovative elements like gecko grippers. This multifaceted approach not only simplifies the mechanical design by eliminating moving parts but also addresses potential risks through redundancy and thorough analysis of thermal and electrical requirements.

D. Structure Subsystem

For the structure of the payload itself, Satellite 6 was chosen by performing a trade study. This is due to its high UTS and Yield strength, as well as its ability to resist thermal fluctuations[12]. In addition, its hardness makes it useful for small debris protection, rather than using larger protection systems such as Whipple shielding[13]. The structure's dimensions are 15.9"x16.5"x13", fitting within the allotted payload volume designated by the Venus Class Bus. The structure of the payload has an estimated mass of 11.834kg. The payload structure must endure several forces, including 7g of axial acceleration[14], 3g of lateral acceleration[14], and 15 Nm of torque. The acceleration forces are the maximum expected launch forces, while the 15 Nm torque is higher than internal reaction wheels can generate. These maximum values were chosen to ensure the payload can survive and still operate in a worst-case scenario. Using SOLIDWORKS, a simulation of these forces can be done. Below are the two launch forces in Fig. 7 and Fig. 8.

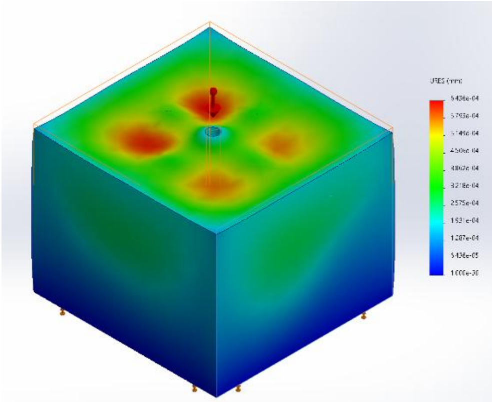

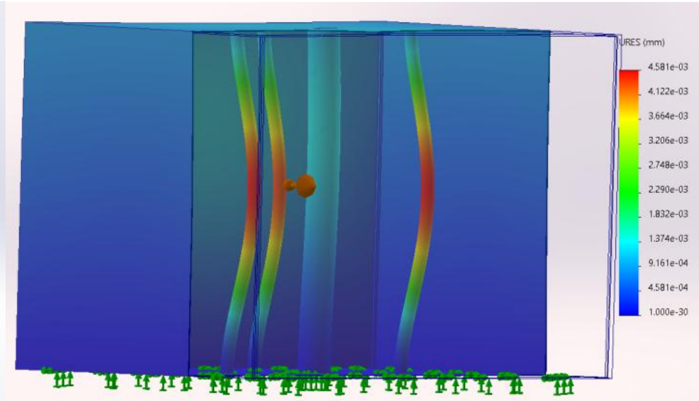

Figure 7. Deformation under 7g of Axial Acceleration.

Figure 8. Deformation of 3g lateral acceleration.

In Fig. 8, the largest deformation is in the supports under 3g of lateral acceleration, about 0.0046 mm. Figure 9 shows the maximum torque case.

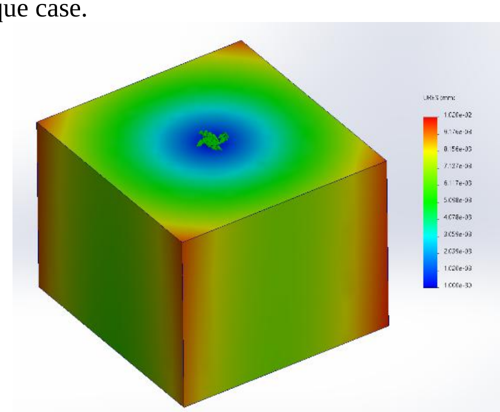

Figure 9. Resultant Displacement of 15 Nm of Torque.

In Fig. 9, the result of the higher-than-maximum torque case is shown. The maximum deflection is around 0.0102 mm, well within allowable and material limits.

E. Command and Data Handling Subsystem

The primary concern for the C&DH subsystem is to ensure that all data required for a successful docking is accurately received and transmitted. To achieve this, the spacecraft must first determine its position, orientation, and location relative to the target. Although star trackers, embedded in the bus, handle initial attitude determination, this section focuses on the sensors used for relative positioning between ATEF and Hubble. After evaluating several sensor options, the team found that each candidate, such as visual and LIDAR systems, has its own strengths and weaknesses. However, relying on a single sensor poses significant risks, so, given the available excess power, volume, and mass, the team opted for multiple redundant sensor solutions. A GPS receiver will aid in initial positioning independently of ground-based radars, though its uncertainty limits render it useless during the actual docking procedure[15]. For the docking process, both LIDAR and visual camera systems will be utilized. Visual systems operate over a larger range and can allow the team to visually verify docking success with the drawbacks of lower positional accuracy and susceptibility to solar interference[15]. While LIDAR provides high-detail data and greater resistance to light pollution, it comes at the expense of a narrower effective range and higher power consumption[15]. As such it was deemed that a combination of all 3 systems would be ideal as it would ensure that the C&DH system is always getting the best data possible.

Table 6. LIDAR Trade Study[15]

Criterion	Weight	ASC GSFL-4K (3D)	Garmin Lidar Lite V3	Ouster OS1
Mass (kg)	0.35	3	0.022	0.43
Normalized Value (Min)		0	1	.8412
Power (W)	0.30	30	0.7	16
Normalized Value (Min)		0	1	.4778
Max Range (m)	0.35	100	40	170
Normalized Value (Max)		.4615	0	1
Total Weighted Score	**1**	.161	.75	.7878

Table 7. Visual System Trade Study[15]

	Weight	IM200	SpectraCAM	AURICAM D80
Mass (Kg)	0.3	0.059	0.18	0.45
Normalized Value (min)		1	0.690537	0
Power Draw (W)	0.2	1	0.4	2
Normalized Value (min)		0.625	1	0
Resolution	0.3	2048x1944	2592X1944	2048x2048
Normalized Value (max)		0	0.201404	1
TRL	0.2	9	8	9
Normalized Value (max)		1	0	1
Total	1	0.625	0.467582	0.5

Table 8. Satellite GPS Trade Study[15]

	Weight	AAC GNSS-701	AerospaceLab GNSS-VSP	Spacemanic Celeste	NovAtel OEM719
Mass (kg)	0.3	0.16	0.394	0.025	0.031
Norm Value (Min)		0.634146341	0	1	0.983739837
Power (W)	0.2	1.8	2.4	0.1	0.9
Norm Value (Min)		0.260869565	0	1	0.652173913
Best Accuracy (m)	0.35	1.5	1.5	2	1.5
Norm Value (Min)		1	1	0	1
Radiation Tolerance (50 given if no destructive event) (krad)	0.15	10	50	40	50
Norm Value (Max)		0	1	0.75	1
TRL		9	9	9	9
Total	1.00	0.592417815	0.5	0.6125	0.925556734

F. Thermal Subsystem

To keep the nitinol docking arm from heating the rest of the payload and bus, a layer of Multi-Layer Insulation (MLI) will be placed between the nitinol and the rest of the craft. The MLI will have an outer layer of Teflon and twenty reflective layers of aluminized mylar. The heat transfer can be found between the MLI and the nitinol by using Eq. (1),

$$Q = \frac{\sigma(T_1^4 - T_2^4)}{\frac{(1-\epsilon_1)}{A_1\epsilon_1} + \frac{1}{A_1F_{1\to2}} + \frac{(1-\epsilon_2)}{A_2\epsilon_2}}\ , \tag{1}$$

where $T_{1,2}$ of the nitinol and satellite are 393.15 K and 283.15 K, respectively, and $\epsilon_{1,2}$ of the nitinol and MLI are 0.66 (Ref. 16) and 0.001221 (Ref. 17), respectively. $A_{1,2}$ of the nitinol and MLI are 0.010125 m^2 and 0.179 m^2, respectively, and $F_{1\text{->}2}$ is 1 since they will be entirely facing each other. This gives a heat transfer of 0.21 watts of power. The MLI's thermal resistance can be used to determine the total temperature change using Eq. (2),

$$R = \frac{1}{A_2\frac{k}{t}}\,, \tag{2}$$

where k of MLI is 0.155 (Ref. 18) and t of the MLI is 0.00254 (Ref. 17). This gives a thermal resistance of 0.0911 K/W, which can convert the 0.21 watts into a change in temperature of about 0.02 K.

IV. Host Payload Integration – Venus Class Bus

A. Structure Subsystem

Assumptions made for the Venus Class Bus were as follows:

- Outer dimensions are 34"x34"x18" (From pixel counts from an image on Blue Canyon Website)
- Material is Aluminum 6061-T6, as it is a very common material for satellites.

Using these assumptions, a rough CAD using SOLIDWORKS of the Venus class bus was produced. This model was tested separately under 7g of axial acceleration and 3g of lateral acceleration. These values were chosen as they are the expected maximum G-forces that a satellite would experience during launch[14]. For both tests, a payload mass of 70kg was set on the top of the Venus Class Bus, where the payload would be placed. The bottom of the Venus Class Bus was fixed, mimicking the attachment to the launch vehicle. The resulting FEA is shown below in Fig. 10 and Fig. 11.

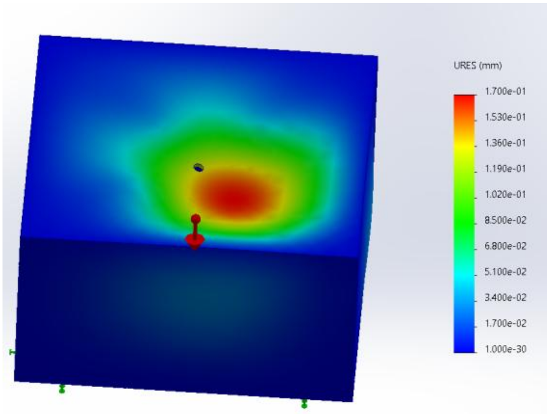

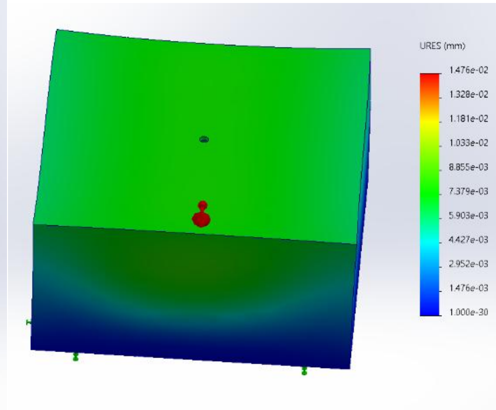

Figure 10. Venus Class Bus Simulated Displacement from 7g Axial Acceleration.

Figure 11. Simulated 3g Lateral Acceleration.

In Fig. 10, most displacement occurs from the axial acceleration. The simulation shows a maximum displacement of about 0.17 mm, while the maximum displacement for the 3g lateral acceleration is around 0.0015 mm. Both displacements are within allowable margins determined by the team. The shell of the Venus Class Bus is estimated to have a mass of 77.401 kg. All walls of the Venus Class Bus are 0.5 inches thick, with 6 supports from the bottom plate to the top plate with 0.5-inch diameter.

B. Command and Data Handling Subsystem

The C&DH Bus subsystem design focuses on establishing reliable data transmission channels from the payload to the bus and ultimately to the ground. Various instruments, such as the GPS transponder, LIDAR sensor, and visual detector (housed in the payload bay), capture the necessary data. Software systems process the raw information into a refined, error-corrected format[15]. To determine the satellite's initial orientation, the bus employs two-star trackers from Blue Canyon Technologies' FlexCore GNC package, chosen for their high reliability and seamless integration[15]. The inclusion of dual star trackers minimizes the risk of a star tracker failing while increasing the overall data quality.

The data processing infrastructure is based on a research paper detailing a magnetic docking demonstration for small satellites conducted by NASA, Blue Canyon Technologies, and several universities[19]. This work, which addresses error correction and proximity detection for novel docking methodologies, closely aligns with ATEF's mission objectives, ensuring that much of the data processing design translates directly to our requirements. Below is one of the data processing flow charts that closely aligns with what ATEF expects to deal with.

Figure 12. Top Level GNC Architecture[19]

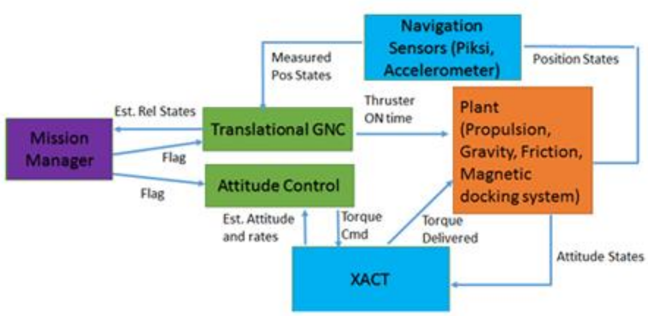

Table 9. C&DH Data Types[20]

Data Type	Description	Relevance to Mission
Command Data	Uplinked instructions from ground control.	Initiates docking, attitude adjustments, software updates.
Telemetry Data	Health and status monitoring of spacecraft subsystems.	Ensures system integrity such as battery voltage, CPU, temperature, pressure
Docking & Maneuvering Data	Real-time position, velocity, and actuator states.	Critical for docking precision and mission success.
Navigation & Attitude Data	Sensor readings for spacecraft orientation.	Ensures stable attitude control (gyroscopes, star trackers).
Fault Detection Logs	System self-checks and automated error recovery.	Enhances system reliability and reduces risk.
Payload & Servicing Data	AOCS software updates and servicing records.	Confirms successful patching of the target satellite.
Ephemeris & Orbit Data	Real-time and predicted satellite trajectory.	Ensures correct orbital placement and adjustments.

Table 10. Data Rate Estimates[20]

Function	Data Size (Kwords)	Execution Frequency (Hz)	Estimated Daily Data (MB)
Command Processing	4.0	10.0	8 MB
Telemetry Processing	2.5	10.0	5 MB
Rate Gyro (Attitude Control)	0.5	10.0	10 MB
Star Tracker (Navigation)	15.0	0.01	1 MB
Reaction Wheel Control	0.3	2.0	2 MB
Thruster Control (Docking)	0.4	2.0	3 MB
Ephemeris Propagation	0.3	1.0	1 MB
Fault Detection (Monitors)	1.0	5.0	3 MB
Software Update Logs	10.0	0.1	5 MB
AOCS Patch Confirmation	2.0	0.05	1 MB
Power & Thermal Monitoring	1.5	10.0	2 MB

C. Thermal Subsystem

To determine the thermal requirements for the payload and bus, Table 11-43 from the 1999 SMAD textbook and each component's datasheet were consulted[19]. While different specific components have varying operational temperature requirements, a rough estimate for the desired internal temperature was found to be about 10 °C (283.15 K).

Tables 11 & 12. Overview of Component Operational Temperature Range.[15, 19]

Component	Typical Temperature Ranges (°C) Operational	Survival
Batteries	0 to 15	−10 to 25
Power Box Baseplates	−10 to 50	−20 to 60
Reaction Wheels	−10 to 40	−20 to 50
Gyros/IMUs	0 to 40	−10 to 50
Star Trackers	0 to 30	−10 to 40
C&DH Box Baseplates	−20 to 60	−40 to 75
Hydrazine Tanks and Lines	15 to 40	5 to 50
Antenna Gimbals	−40 to 80	−50 to 90
Antennas	−100 to 100	−120 to 120
Solar Panels	−150 to 110	−200 to 130

Specific Part Name	Operating temp (C)
Ibeos Modular Power System	-35 to 60
LG-MJ1 Battery	0 to 45
FleXcore	-20 to 60
NovAtel OEM719	-40 to 85
Ouster OS1	-40 to 60
IM200	-20 to 40
N2H4 tanks	~20
Kevlar	-40 to 200
Nitinol	-20 to 130

The next consideration is the temperature effect from the environment. After using the scale image of the Venus class bus from Blue Canyon's website, it was estimated that the bus would be a box of dimensions 34" x 34" x 18". Additionally, using the payload base dimensions from the RFP, the surface area that would be affected by the Sun and Earth is roughly 3.3 m^2. The amount of energy input from the environment around the satellite can be found using equations (1), (2), (3), and (4),

$$q_{solar} + q_{albedo} + q_{IR} + Q_{gen} = Q_{stored} + Q_{out,rad} \tag{1}$$

$$q_{ir} = \sigma\varepsilon A F_{earth\text{->}surface} (T_E^4) \tag{2}$$

$$q_{albedo} = \alpha A S A_f F_{earth\text{->}surface} \tag{3}$$

$$q_{solar} = \alpha A S \cos(\theta) \tag{4}$$

from Ref. 15 and Ref. 21. For the absolute worst-case scenario, the view factor and incident angle are assumed to be 1 and 0, as those cause the most amount of power input into the satellite. The bus will be surrounded by MLI, which will have Teflon outer cover and twenty reflective layers of aluminized mylar. This will give the surface of the bus an effective emissivity and absorptivity of 0.001221 and 0.003419, respectively[17]. Using these equations, the total power flowing into the satellite was found to be about 21.05 Watts. Using the 444 Watts of internally generated power from the payload and bus, the total amount of power needing to be dissipated to ensure thermal neutrality is roughly 465.05 Watts. Using equation (5) from Ref. 21,

$$Q_{out,rad} = A\varepsilon\sigma T_4 \tag{5}$$

the power passively radiated from the satellite can be estimated to be about 1.5 watts.

To dissipate this amount of power, a trade study on a few deployable radiators was done. The three determining factors were radiated power in terms of W/m^2, density in terms of kg/m^2, and TRL. The best radiator was determined to be Thermal Management Technologies' deployable radiator[22]. According to their website, this radiator currently only has a TRL of 6, however it is the highest available on the market for this size of satellite.

Using two of these radiators with a surface area of about 0.42 m^2 each, the bus can radiate about 463 Watts. This, combined with the passive radiation previously found, shows that a total of about 465 Watts is now radiated from the satellite. These two radiators have a total mass of about 6.7 kg.

D. Power Subsystem

When designing the mission's power subsystem, it was crucial to know how much power the satellite will be utilizing while it is on the dark side of the Earth and how much power the satellite can obtain while on the light side of the Earth. Assuming the payload is always using all 444 Watts of power during this period and using eclipse data obtained from the Orbital Analysis subsystem (which used STK's eclipse timing calculator), it is found that the satellite would require 265.4 Watt-hours while in parking orbit and 265.1 Watt-hours during nominal operations. As it is using 444-Watt solar panels and using the eclipse data, it is found that the satellite can get a total of 434.7 Watt-hours while in parking orbit and 441.0 Watt-hours during nominal operations. This gives lower and upper bounds for the Watt-hours needed when determining which batteries to use.

Within Ref. 15, five batteries were determined to be viable. A trade study was conducted, prioritizing the specific energy, volumetric energy density, and their typical capacity. Due to the very limited mass allowed, specific energy was given far more weight than the other two factors. This trade study resulted in choosing LG Chem's LG MJ1 (3500mAh) battery. According to Ref. 15, the LG MJ1 has flight heritage with NASA's PACE mission, so it is estimated to have a TRL of 9. Each LG MJ1 battery is 49 grams with 12.74 Watts each[23], so that gives 440 Watt-hours of energy from 35 batteries, taking up 1.715 kg and about 624.4 cm^3.

To manage and distribute this power, a Power Management and Distribution (PMAD) system is needed. After looking through Ref. 15, several PMAD systems were chosen for a trade study. Mass and volume were considered large factors due to the mission's limitations in those areas. This trade study resulted in choosing Ibeos's Modular EPS, which takes up about 1 kg and about 1150 cm^3 [24]. This gives a total mass and volume of about 2.715 kg and 1774.4 cm^3 for the power subsystem, respectively.

E. Communication Subsystem

To ensure robust and continuous communication throughout the mission, a complete trade study and link budget analysis were conducted for both uplink and downlink operations in the S-band. The process began with a detailed evaluation of multiple antenna candidates based on gain, power consumption, latency, polarization, mass, and flight heritage. Each antenna was normalized across these metrics and scored using a weighted matrix to ensure objective and mission-driven selection.

1. Antenna Trade Study

A comparative evaluation of multiple S-band antennas was performed based on gain, power consumption, latency, polarization, mass, and flight heritage[15]. The IQ Spacecom Single Patch Antenna emerged as the optimal solution, achieving the highest final score of 0.743. It offers a moderate gain of 6 dBi, suitable for LEO communication links, while maintaining a low power requirement of just 1 watt[25], which is critical for this power-constrained satellite mission. Its circular polarization minimizes polarization mismatch losses with ground stations, improving link reliability regardless of spacecraft orientation. Additionally, it features a compact footprint and low mass (49 g)[25,26], easing integration without impacting the spacecraft's mass or volume margins. Importantly, the antenna has proven flight heritage, having been used successfully on previous space missions, an essential factor in minimizing risk and improving confidence in on-orbit performance.

2. Downlink/Uplink Analysis

For the downlink, the spacecraft transmits telemetry and science data to the Santiago Ground Station, which features an 11-meter high-gain antenna[27]. The system operates at 2.025 GHz with a transmit power of 1 W and a data rate of 100 kbps. A path length of 2,697.5 km and system noise temperature of 50.01 K were used in the analysis, along with a total propagation and polarization loss of -0.3 dB. The link budget simulation in STK yielded a signal-to-noise ratio (SNR) of 4.50 dB and a final link margin of 2.84 dB, confirming the downlink's reliability under nominal and degraded conditions.

The uplink supports command and control transmission from ground to spacecraft. Operating at 2.025 GHz, the ground station provides sufficient EIRP using a high-power transmitter and the same 11-meter antenna (48.3 dBi gain). The spacecraft's receiving antenna, with 6 dBi gain, was analyzed over the same 2,697.5 km path length. A system noise temperature of 290 K and a lower data rate of 10 kbps ensured robust performance. The analysis returned an SNR of 6.00 dB and a link margin of 3.10 dB, ensuring command signals are reliably received even in less-than-ideal conditions.

F. Attitude Subsystem

A comprehensive trade study was conducted to evaluate commonly used integrated Attitude Determination and Control Systems (ADCS) for potential mission implementation. The systems considered in the analysis included XACT-15, XACT-50, XACT-100, and FleXcore. Each option was assessed based on four primary criteria: pointing accuracy, momentum storage, Technology Readiness Level (TRL), and mass. These criteria were selected to capture both the performance capabilities and practical integration aspects of the systems.

From a mission perspective, pointing accuracy and momentum storage were identified as the most critical parameters. High pointing accuracy is essential for maintaining precise alignment with mission targets, particularly for operations such as docking, and was therefore given the highest weight of 0.4. Momentum storage was assigned a weight of 0.3, as it directly influences the spacecraft's ability to maintain and adjust its orientation over time. TRL received a weight of 0.2 to ensure the selected system could perform consistently in operational environments. Mass was considered less critical and was weighted as 0.1.

Following this weighted evaluation approach, FleXcore achieved the highest overall score of 0.70. While its TRL of 8 is slightly lower than that of some other candidates rated at TRL 9, FleXcore's superior technical performance, specifically its pointing accuracy of 0.002° and momentum storage capacity of 8 Nms proved decisive in the selection process. These advantages were considered sufficient to outweigh the marginal difference in TRL. FleXcore’s TRL 8 designation is supported by its successful deployment in multiple flight missions. The system has demonstrated reliable in-space performance on operational satellites launched aboard Falcon 9 missions, including Transporter-5 and Transporter-6, thereby confirming its flight-proven heritage[28-30]. In addition, FleXcore has consistently delivered high-precision attitude control and stable momentum storage across a range of mission conditions, validating its performance under operational stress[31]. Its integration into commercial, defense, and scientific missions further reinforces its readiness and adaptability to various orbital environments[29]. These factors collectively confirm FleXcore’s maturity and reliability, supporting its selection as the optimal ADCS for the mission.

G. Propulsion Subsystem

For propulsion, two systems were selected via trade studies. For the main hot gas propulsion system, MONARC-5 was chosen. For the cold gas propulsion system, the B1 by Dawn Aerospace was selected. MONARC-5 was selected due to its thrust capabilities, as well as low mass and volume[32]. The power requirements were also low, and it had a TRL of 9 [32]. The B1 cold gas thruster was selected due to its ability to act as both a cold gas and hot gas thruster. By powering an igniter, the thruster turns into a hot gas thruster, increasing its thrust from 0.49 newtons to 1.35 newtons. In addition, B1 has low mass, low volume requirements, and a TRL of 9 [33]. One important consideration for close-proximity maneuvers was the likeliness of leaving a residue. The cold gas mixture for B1 is N2O and C3H6, both of which are very unlikely to leave a residue in the LEO environment[34,35]. To move from a parking orbit of 500 km to Hubble’s orbit of 515km, around 3 kg of hydrazine would be necessary. To assist in deorbiting Hubble from 515 km to 300 km, much more would be required. Due to this, 40 kg of hydrazine will be equipped onboard, allowing both maneuvers with extra propellant for risk mitigation and safety reasons. This amount of hydrazine requires a tank volume of approximately 39,821 cm^3 [36]. The mission also will carry a combined 10 kg of B1 propellant mixture. Assuming stoichiometric burning, this requires 6.806 kg of N2O and 3.25 kg of C3H6. The propellant tanks were assumed to be cylindrical midbodies with hemispherical ends. This means that the volume of the tank is simply the volume of a cylinder plus the volume of a sphere. The height of the cylinder for all three tanks was set to 10 cm. Table 13 shows the breakdown of tank properties.

Table 13. Tank Properties for Propellants.

Propellant	Mass (kg)	Density (kg/m^3)	Volume Required (cm^3)	Radius (cm)	Thickness Required (cm)
N2O	6.806	1230.452	5531.3	9	1
C3H6	3.25	610.065	5327.3	9	1
Hydrazine	40	1004.49991	39820.81	19	2

The density of N_2O[34] and C_3H_6[35] were assumed from the standard temperature and pressure of each. The thickness requirement was based on a maximum hoop stress of 1/4th of yield strength of Aluminum 6061-T6, which was the selected material for the storage tanks.

H. Launch Vehicle

To determine the optimal launch vehicle for the mission, a comprehensive trade study was conducted. This trade study included five launch vehicles: Falcon 9 (SpaceX), Electron (Rocket Lab), Vega-C (Arianespace), Minotaur IV (Northrop Grumman), and Minotaur I (Northrop Grumman). The assessment was based on four key criteria including reliability based on the success rate, cost per launch, fairing volume, and payload mass to low earth orbit. Each criterion was assigned a weight based on the belief of its significance to the mission. To weigh the options, a normalized value was calculated to provide a fair comparison among launch options.

The results of the trade study indicated that Falcon 9 scored the highest in overall suitability. To go through the criteria, it showed a success rate of 99.74%. The fairing volume of around 67.8 m^3 far exceeded that of the other launch vehicles, ensuring plenty of space for the payload[2]. Falcon 9's capacity of 22,800 kg to low earth orbit was also substantially higher than the alternatives[2]. Based on these criteria, Falcon 9 received the highest normalized score of 0.6942, making it the most optimal choice for the mission.

To combat the high cost of Falcon 9 launches, Team Osiris opted for a rideshare approach to maximize cost efficiency. The decision to use rideshare was further supported by industry trends and NASA initiatives, as highlighted in the provided documentation, "Growing Rideshare Market: The demand for rideshare missions has increased due to the rising number of SmallSats and CubeSats seeking affordable launch options"[15]. By sharing launch costs with other payloads, the mission achieves a lower per-kilogram cost compared to a dedicated launch, estimating the cost of launch for the Falcon 9 down from 69 million to 1-5 million.

In the outcome that Falcon 9 cannot be used due to differences in mission requirements, Team Osiris has agreed to fall back on Electron from Rocket Labs which has output a normalized score of 0.344. While this is the third best normalized score, the team believes this rocket suits the mission the second best, after Falcon 9.

I. Ground Station

A detailed trade study was conducted to identify the optimal ground stations[27,37-39] for reliable communication with the spacecraft in Hubble's orbit. Stations were evaluated across five weighted criteria: Hubble Pass Frequency (35%), Orbital Coverage Alignment (30%), S-band Capability (20%), Antenna Infrastructure (10%), and Weather Reliability (5%). The analysis concluded with Santiago[27] and Hawaii[39] Ground Stations as the top candidates, scoring 0.85 and 0.80 respectively.

Santiago Ground Station was selected as the primary node due to its strong alignment with Hubble's orbit, high pass frequency, existing S-band support at 2.2 GHz, and robust infrastructure, including 9 m to 13 m antennas. It supports 5–6 passes per day with 10–15 minutes of visibility per pass and maintains a low signal delay of 3 ms. Its moderate weather conditions and flight-proven reliability further solidify its role[27]. Hawaii Ground Station was chosen as a backup to ensure continuous coverage. It offers similar visibility, strong infrastructure, and reliable S- and Ku-band support[39]. With a stable climate and strong NASA heritage, it complements Santiago by filling coverage gaps when the primary station is out of view. Together, these stations provide a redundant and reliable ground network for the mission, minimizing communication downtime and ensuring consistent telemetry and command access.

J. Orbital Analysis

The mission's orbital design prioritizes cost efficiency, safety, and operational flexibility. The selected strategy involves deploying the payload into a 500 km circular parking orbit, followed by a Hohmann transfer to Hubble's 515 km orbit under matching inclination and orbital conditions. This approach was chosen after evaluating trade-offs in launch feasibility, system verification, and delta-v requirements.

Using a 500 km parking orbit offers several key advantages over a direct insertion into Hubble's orbit. First, it increases launch flexibility by expanding available launch windows and vehicle options, while also enabling compatibility with rideshare missions, reducing launch costs from $69 million for a dedicated mission to approximately $1-5 million[19,40]. Second, it enhances safety by allowing system verification away from Hubble, minimizing the risk of failures near the telescope. The parking orbit also acts as a safe fallback zone in the event of payload anomalies[19]. Although this method introduces an additional maneuver, the delta-v penalty is only 8 m/s compared to the operational and financial benefits it provides[19].

Following system checkout, the payload will execute a Hohmann transfer to reach Hubble's orbit. This maneuver was selected for its delta-v efficiency, simplicity, and reliability. As the most fuel-efficient option for small altitude changes, the Hohmann transfer reduces propellant consumption while also minimizing computational complexity and execution risk[19].

Once at Hubble's altitude, the payload will experience periodic eclipses, which are critical for power and thermal management. STK simulations indicate that approximately 35% of each orbit will be spent in eclipse, with variations depending on Earth's axial tilt and orbital position relative to the Sun[19].

In summary, the combination of a 500 km parking orbit and a Hohmann transfer represents the optimal balance between cost, safety, and performance. The approach minimizes risk, reduces mission cost through rideshare opportunities, and ensures a controlled and efficient transition to Hubble's orbit, with only a negligible delta-v trade-off.

K. Risk and Fault Recovery

1. Risk Management

Table 14. Risks and Mitigation Strategy.

	Risks	Mitgation Stratagy
1	Solar heating causes premature docking	The inclusion of multiple thermal barriers between the sun and nitinol, as well as pointing the docking claw away from the sun until docking, greatly minimizes the chance of an uncontrolled nitinol activation.
2	Failed dock attempt	The inclusion of undocking bands in the nitinol docking clamp enables multiple docking attempts with some downtime between each.
3	Impacting target satellite on rendezvous & docking	Engage the B1 igniters to boost the thrusters' thrust capabilities, enabling maneuvers away from the target satellite. Additionally, incorporate a combination of sensors to ensure accurate positioning data.
4	Nitinol docking clamp fails to completly arrest target and payload	Incorporating gecko grippers into the docking claw vastly decreases the likelihood of sliding.
5	Target reducing effectiveness of ATEF's solar pannels	A surplus of power is built into the payload's design to mitigate the impact of lower-than-expected sun exposure.

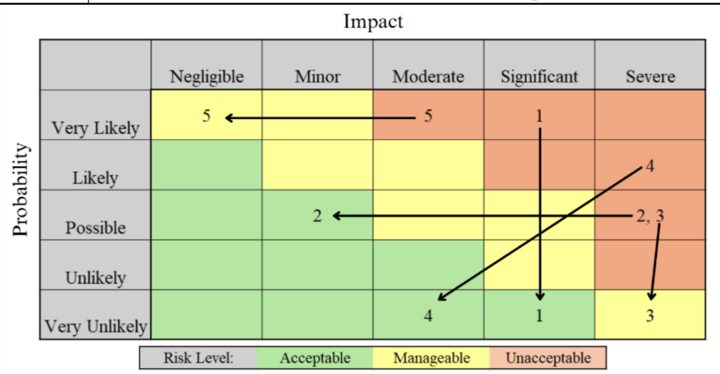

Figure 13. Risk Mitigation Matrix.

2. Fault Recovery Plans

The first major fault considered was the potential for the nitinol docking bands to be damaged or restricted during launch, preventing proper deployment. This fault would be caught during systems test, Action 6 of the general mission plan, when the nitinol docking clamps are evaluated. If the fault occurs, the mission would be descoped to rely solely on gecko grippers for docking. However, this change could potentially require shifting the dock position and imposing stricter limits on maximum momentum or thrust applied to Hubble, to reduce strain on the docking system. Although the damage to the nitinol docking clamp would be detrimental, the mission could still proceed, albeit with slower attitude changes.

The second major fault considered was damage to a solar panel during docking, either from thruster outgassing or a collision with the target. Such damage would be immediately evident as a noticeable power drop and would be identified during the visual inspection of dock integrity (Action Item 15 on the payload-specific mission plan). Although the short-term effects might be limited, losing a solar panel would eliminate the mission's built-in design surplus, potentially forcing some systems to be powered off to conserve energy. This reduction in available power could compromise the overall performance of ATEF, in turn shortening the mission's duration from years to only a few months. So, while ATEF could still demonstrate the feasibility of its design proving the idea, its mission would be cut short.

L. Future Work

Future work will focus on refining key subsystems. For docking, efforts include quantifying the impact of Kevlar and MLI layers via full finite element analysis, conducting detailed thermal assessments for repeated eclipse cycles, and further integrating gecko grippers, with a real-world high-fidelity prototype. The payload structure will be optimized by exploring a pre-built chassis concept and adding internal supports to better model lateral and axial forces while trimming down weight. Simultaneously, the Venus Class Bus design will be improved to reduce structural mass and enhance the accuracy of its internal layout.

The C&DH subsystem will undergo extensive radiation analysis to estimate mission duration and assess the necessity of an atomic clock for attitude adjustments, while hardware selections will prioritize robust and well-shielded components. Detailed, component-specific thermal calculations will be used to fine-tune radiator and heater requirements, and power subsystem efforts will ensure that voltage and current needs are met through optimal battery configurations. Additionally, communication challenges such as latency, signal delay, and the performance of the IQ Spacecom Single Patch Antenna will be addressed, with research into higher data rates balancing power, bandwidth, and processing constraints.

Further work will also refine the propulsion aspects by calculating the cold gas propellant needed for docking maneuvers and improving launch vehicle assessments by comparing real-world performance against reliability metrics to better estimate costs. Enhanced CAD efforts will increase design fidelity through refined finite element analysis, integrating precise material properties and load conditions to optimize structural strength and weight. Finally, comprehensive mass and power calculations will be iterated as subsystems are finalized, and a test maneuver will be planned to validate the integrated system.

V. References

[1] *Mev-1 & 2 (mission extension vehicle-1 and -2) - eoportal* Available: https://www.eoportal.org/satellite-missions/mev-1.

[2] *FALCON USERS GUIDE SpaceX* Available: https://www.spacex.com/media/falcon-users-guide-2021-09.pdf.

[3] *NASA's Hubble Pauses Science Due to Gyro Issue (2024) NASA*. Available at: https://science.nasa.gov/missions/hubble/nasas-hubble-pauses-science-due-to-gyro-issue/

[4] *Hubble Space Telescope 3D model (2019) NASA*. Available at: https://science.nasa.gov/resource/hubble-space-telescope-3d-model/

[5] *Gianopoulos, A. (2022) NASA, spacex to study Hubble Telescope Reboost Possibility, NASA*. Available at: https://www.nasa.gov/missions/hubble/nasa-spacex-to-study-hubble-telescope-reboost-possibility/.

[6] *Plates and sheets (2025) Kellogg's Research Labs.* Available at: https://www.kelloggsresearchlabs.com/product/nitinol-plates/.

[7] *Nitinol Technical Properties (no date) MDC*. Available at: https://www.medicaldevicecomponents.com/resource-library/principles-of-nitinol/nitinol-technical-properties/.

[8] *Nitinol technical basic FAQ (no date) Kellogg's Research Labs*. Available at: https://www.kelloggsresearchlabs.com/nitinol-faq/.

[9] *Landau, E.R. (2015) Gecko grippers moving on up, NASA*. Available at: https://www.nasa.gov/missions/station/gecko-grippers-moving-on-up/.

[10] *Kevlar® Aramid Fiber Technical Guide (no date) DuPont*. Available at: https://www.dupont.com/content/dam/dupont/amer/us/en/safety/public/documents/en/Kevlar_Technical_Guide_0319.pdf.

[11] *The Red Book (no date) Sheldahl*. Available at: https://sheldahl.com/wp-content/uploads/2023/07/RedBook.pdf.

[12] *STELLITE® 6 ALLOY (no date) Deloro Stellite*. Available at: http://specialmetals.ir/images/technical_info/cobalt_base/Stellite_6.pdf.

[13] *Stellite alloy 6 (UNS R30006) (no date) AEETHER*. Available at: https://www.aeether.com/AEETHER/grades/6.html.

[14] *What G-forces do different launchers cause? (2015) Stack Exchange*. Available at: https://space.stackexchange.com/questions/6461/what-g-forces-do-different-launchers-cause.

[15] *Weston, S.V. et al. (2025) State-of-the-Art Small Spacecraft Technology , NASA*. Available at: https://nasa.gov/wp-content/uploads/2025/02/soa-2024.pdf?emrc=0945a0.

[16] *Wei-Yu Feng et al. (no date) MEDUSA – Mechanism for Entrapment of Debris Using Shape memory Alloy, MEDUSA*. Available at: https://conference.sdo.esoc.esa.int/proceedings/sdc7/paper/487/SDC7-paper487.pdf.

[17] Finckenor, M.M. (1999) Multilayer Insulation Material Guidelines, NASA. Available at: https://ntrs.nasa.gov/api/citations/19990047691/downloads/19990047691.pdf.

[18] *DuPont Teijin Films Mylar® A Polyester Film, 500 Gauge (no date) MatWeb*. Available at: https://www.matweb.com/search/datasheet_print.aspx?matguid=981d85aa72b0419bb4b26a3c06cb284d.

[19] *James Richard Wertz and W. J. Larson, (1999) Space Mission Analysis and Design, 3rd ed., vol. 3*.

[20] *Pei et al., "Ground Demonstration on the Autonomous Docking of Two 3U Cubesats Using a Novel Permanent-Magnet Docking Mechanism," NASA*. Available at: https://ntrs.nasa.gov/api/citations/20170001226/downloads/20170001226.pdf

[21] *Small Satellite Thermal Modeling Guide (2022) AFRL*. Available at: https://apps.dtic.mil/sti/trecms/pdf/AD1170386.pdf.

[22] *Thermally Efficient Deployable Radiators (2021) TMT*. Available at: https://www.tmt-ipe.com/_files/ugd/4ab2a3_a6491d821ff84523b1ad6026c3c1213c.pdf?index=true.

[23] *Lee, K. hee (2016) PRODUCT SPECIFICATION Rechargeable Lithium Ion Battery Model : INR18650 MJ13500mAh, LG Chem*. Available at: https://cdn.shopify.com/s/files/1/0721/2761/1190/files/IMR_18650_3000_40A.pdf?v=1714072750.

[24] *Modular Power System (no date) Ibeos*. Available at: https://www.ibeos.com/modular-power-system.

[25] *S Band Patch Antenna Interface Control Document (2024) Spacecom.* Available at: https://www.iq-spacecom.com/images/images/shop/datasheets/202173--03-90.pdf.

[26] *S-band Antenna - IQ SPACECOM (no date) SmallSat Catalog*. Available at: https://catalog.orbitaltransports.com/s-band-antenna-iq-spacecom/.

[27] *Santiago station (no date) SSC*. Available at: https://sscspace.com/services/satellite-ground-stations/our-stations/santiago-station/.

[28] *Blue Canyon Technologies Deploys Multiple Components Aboard Falcon 9 Launch (2021) Business Wire*. Available at: https://www.businesswire.com/news/home/20210125005419/en/Blue-Canyon-Technologies-Deploys-Multiple-Components-Aboard-Falcon-9-Launch.

[29] *Blue Canyon Technologies Provides Multiple Spacecraft Aboard Transporter-5 Launch (2022) Blue Canyon Technologies.* Available at: https://www.bluecanyontech.com/news/blue-canyon-technologies-provides-multiple-spacecraft-aboard-transporter-5-launch/.

[30]*Blue Canyon Technologies provides small satellite critical T (2023) Blue Canyon Technologies Provides Small Satellite Critical T*. Available at: https://www.asdnews.com/news/aerospace/2023/01/10/blue-canyon-technologies-provides-small-satellite-critical-technologies-transporter6-launch.

[31]B*lue Canyon's low-altitude smallsats thrive on-orbit after their launch via SpaceX's Transporter-5 mission (2022) SatNews*. Available at: https://news.satnews.com/2022/06/05/blue-canyons-low-altitude-smallsats-thrive-on-orbit-after-their-launch-via-spacexs-transporter-5-mission/.

[32]*Moog (no date) 5 N Monopropellant Thruster for Space Exploration Missions, SatNow*. Available at: https://www.satnow.com/products/thrusters/moog/36-1152-monarc-5.

[33]D*awn Aerospace (no date) Cold Gas Thruster for Customized Propulsion Systems, SatNow*. Available at: https://www.satnow.com/products/thrusters/dawn-aerospace/36-1161-b1.

[34]*Nitrous oxide (no date) Gas Encyclopedia Air Liquide*. Available at: https://encyclopedia.airliquide.com/nitrous-oxide#properties.

[35]*Propene (no date) Gas Encyclopedia Air Liquide.* Available at: https://encyclopedia.airliquide.com/propene#properties.

[36] *Calculate volume of compounds and materials per weight (no date) Aqua Calc.* Available at: https://www.aqua-calc.com/calculate/volume-to-weight.

[37]M*adrid Deep Space Communications Complex DEEP SPACE NETWORK (2024) NASA*. Available at: https://www.mdscc.nasa.gov/.

[38]G*oldstone Deep Space Communications Complex (no date) NASA.* Available at: https://www.gdscc.nasa.gov/.

[39]*Ground Stations (no date) HSFL*. Available at: https://www.hsfl.hawaii.edu/ground-stations/.

[40]*Smallsat Rideshare Program (no date) SpaceX*. Available at: https://www.spacex.com/rideshare/.